

# SHIFTING FUNDAMENTALS: SCALING RELATIONS INVOLVING NUCLEAR STAR CLUSTERS AND SUPERMASSIVE BLACK HOLES

NICHOLAS SCOTT AND ALISTER W GRAHAM

Centre for Astrophysics and Supercomputing, Swinburne University of Technology, Hawthorn, Vic, 3122, Australia  
*Draft version November 30, 2019*

## ABSTRACT

We investigate whether nuclear star clusters and supermassive black holes follow a common set of mass scaling relations with their host galaxy’s properties, and hence can be considered to form a single class of central massive object. We have compiled a large sample of galaxies with measured nuclear star cluster masses and host galaxy properties from the literature and fit log-linear scaling relations. We find that nuclear star cluster mass,  $M_{\text{NC}}$ , correlates most tightly with the host galaxy’s velocity dispersion:  $\log M_{\text{NC}} = (2.11 \pm 0.31) \log(\sigma/54) + (6.63 \pm 0.09)$ , but has a slope dramatically shallower than the relation defined by supermassive black holes. We find that the nuclear star cluster relations involving luminosity, mass and dynamics, intercept with but are in general shallower than the corresponding black hole scaling relations. In particular  $M_{\text{NC}} \propto M_{\text{Gal,dyn}}^{0.55 \pm 0.15}$ , whereas  $M_{\text{BH}} \propto M_{\text{Gal,dyn}}^{1.37 \pm 0.23}$  for our sample of massive black holes when fit with a single power-law. We also find that the nuclear cluster mass is *not* a constant fraction of it’s host galaxy’s or spheroid’s mass. We conclude that nuclear stellar clusters and supermassive black holes do not form a single family of central massive objects.

*Subject headings:* galaxies: dwarf — galaxies: fundamental parameters galaxies: kinematics and dynamics — galaxies: nuclei — galaxies: star clusters — galaxies: structure —

## 1. INTRODUCTION

Central massive objects (CMOs) are a common feature in galaxies across the Hubble sequence. CMOs take the form of either a supermassive black hole (SMBH) or a compact stellar structure such as a nuclear stellar cluster (NC) or nuclear stellar disk (ND). The masses of SMBHs have been shown to correlate with a range of host galaxy properties including: stellar velocity dispersion,  $\sigma$  (Ferrarese & Merritt 2000; Gebhardt et al. 2000; Graham et al. 2011), stellar concentration (Graham et al. 2001; Graham & Driver 2007); dynamical mass,  $M_{\text{dyn}} \propto \sigma^2 R$  (Magorrian et al. 1998; Marconi & Hunt 2003; Häring & Rix 2004; Graham 2012a); and luminosity,  $L_{\text{Sph}}$  (Kormendy & Richstone 1995; Marconi & Hunt 2003; Sani et al. 2011).

More recently, following the discovery that the luminosity of stellar CMOs correlates with that of their host bulge in disk galaxies (Balcels et al. 2003, 2007) and elliptical galaxies (Graham & Guzmán 2003), the *masses* of stellar CMOs have also been shown to correlate with their host galaxy properties. NC mass has been reported to correlate with, for early-type galaxies, the host *galaxy’s* luminosity,  $L_{\text{Gal}}$  and dynamical mass, as given by  $M_{\text{Gal,dyn}} \propto \sigma^2 R_{\text{e,Gal}}$  (Ferrarese et al. 2006a). Related correlations have also been reported with the host *spheroid’s* luminosity,  $L_{\text{Sph}}$  (Wehner & Harris 2006); stellar mass,  $M_{\text{Sph,*}}$  (Balcels et al. 2007); dynamical mass,  $M_{\text{Sph,dyn}}$  (Wehner & Harris 2006; Balcels et al. 2007), and velocity dispersion,  $\sigma$  (Ferrarese et al. 2006a; Graham 2012b).

These scaling relations are physically interesting because they relate objects on very different scales: the gravitational sphere of influence of a SMBH is typically less than 0.1 per cent of its host galaxy’s effective radius,  $R_{\text{e}}$ . This connection is thought to be driven by feed-

back processes from the CMO (e.g. Silk & Rees 1998; Croton et al. 2006; Booth & Schaye 2009), but may instead be related by the initial central stellar density of the host spheroid (Graham & Driver 2007). While most studies have focused on feedback from black holes, analogous mechanisms driven by nuclear stellar clusters have been hypothesized (King 2005; McLaughlin et al. 2006; McQuillin & McLaughlin 2012). One problem with these momentum-conserving feedback arguments, as constructed, is that they predict a slope of 4 for both the  $M_{\text{BH}}-\sigma$  and  $M_{\text{NC}}-\sigma$  relations, whereas the observations now suggest a slope of 5 (Ferrarese & Merritt 2000; Graham et al. 2011) and somewhere between 1 and 2 (Graham 2012b), respectively. At least for the  $M_{\text{BH}}-\sigma$  relation, energy conserving arguments predict a slope of 5 (Silk & Rees 1998).

Ferrarese et al. (2006a, hereafter F06) and Wehner & Harris (2006, hereafter WH06) have argued that SMBHs and NCs follow a single common scaling relation with  $M_{\text{dyn}}$  (though not with other host galaxy properties). Other investigations have reached different conclusions, for example Balcels et al. (2007, hereafter BGP07) find that NCs do not fall onto the same linear relation as defined by more massive central black holes, and conclude that any CMO–bulge mass relation that encompasses both central black holes and nuclear star clusters must not be log-linear.

F06 have reported that the  $M_{\text{NC}}-\sigma$  relation has a slope which is consistent with the  $M_{\text{BH}}-\sigma$  relation. However expanding upon the  $M_{\text{CMO}}-\sigma$  diagram from Figure 8 of Graham et al. (2011), Graham (2012b) has reported that  $M_{\text{NC}} \propto \sigma^1$  to  $\sigma^2$ , whereas  $M_{\text{bh}} \propto \sigma^5$  for non-barred galaxies<sup>1</sup> (Ferrarese & Merritt 2000;

<sup>1</sup> Barred galaxies tend to have higher velocity dispersions than

Graham et al. 2011).

The situation is complicated still further by a blurring of the division between galaxies containing SMBHs or NCs. Since F06, and WH06 who initially found a clear division in mass between galaxies hosting a SMBH (with  $M_{\text{Sph,dyn}} > 5 \times 10^9 M_{\odot}$ ) and galaxies hosting a NC (with  $M_{\text{Sph,dyn}} < 5 \times 10^9 M_{\odot}$ ), an increasing number of galaxies that host both a SMBH and a NC have been found (Graham & Driver 2007; González Delgado et al. 2008; Seth et al. 2008). Graham & Spitler (2009, hereafter GS09) observed a transition region from  $10^8 < M_{\text{sph,*}}/M_{\odot} < 10^{10}$  where both types of nuclei coexist (see also Neumayer & Walcher 2012). These findings raise the question how the combined CMO mass,  $M_{\text{BH}} + M_{\text{NC}}$ , may scale with the host galaxy properties, though a larger sample of such objects is desired.

Graham (2012b) updated the  $M_{\text{CMO}}-\sigma$  diagram, first published by F06, using an expanded sample of galaxies with directly measured SMBH masses which also included 13 galaxies with both a NC and SMBH. Here we re-examine and update the  $M_{\text{CMO}}$  versus velocity dispersion,  $B$ -band galaxy magnitude and dynamical mass diagrams from F06. In addition to the above sample expansion, we also incorporate the NC data set from Balcells et al. (2007). We also construct another three diagrams involving  $M_{\text{CMO}}$  and:  $K$ -band luminosity; total stellar mass,  $M_{\text{Gal,*}}$ ; and spheroid stellar mass,  $M_{\text{Sph,*}}$ .

Collectively our data represents the largest sample to date of NC and host galaxy properties. We have used this to investigate their scaling relations and whether they are consistent with those for SMBHs. Our sample and data are more fully described in Section 2, while in Section 3 we present a range of NC and SMBH scaling relations. In Section 4 we discuss whether our results support the idea of a single common scaling relation for CMOs and what expectations we have from theories of galaxy formation and growth. Finally we present a summary of our conclusions at the end of Section 4.

## 2. SAMPLE AND DATA

We constructed our sample of nuclear stellar objects by combining the data from F06 (51 objects, 29 with measured  $\sigma$ ), BGP07 (17 objects, all with measured  $\sigma$ ) and GS09 (16 objects, 13 with measured  $\sigma$ ). Graham (2012b) added a further 3 objects (with measured  $\sigma$ ) to the GS09 sample for a total of 19 objects, 15 with both a NC and a SMBH and a further 4 objects with a NC and only an upper limit on  $M_{\text{BH}}$ . This gives a final sample of 87 objects with measured  $M_{\text{NC}}$ , 62 of which have a measurement of  $\sigma$ . Our sample of BH galaxies is taken from Graham et al. (2011) and consists of 64 objects, all with measured  $\sigma$  and  $M_{\text{BH}}$ .

### 2.1. Nuclear stellar masses

GS09 provide stellar masses for their nuclei, whereas F06 and BGP07 tabulate only magnitudes. For the F06 objects we derived nuclear stellar object masses following F06. We multiplied the total galaxy  $g$ -band magnitude by a mass-to-light ratio,  $M/L$ , determined from the single stellar population models

given by the  $M_{\text{BH}}-\sigma$  relation defined by non-barred galaxies (Graham 2008; Hu 2008)

Bruzual & Charlot (2003), using the nuclear cluster colors given in Côté et al. (2006) and a stellar population age  $t = 5$  Gyrs. For the BGP07 objects we derived masses following BGP07, by multiplying the total galaxy  $K$ -band magnitude by  $M/L_K = 0.8$  (Bell & de Jong 2001) based on typical colors of the bulge population. The uncertainties on the nuclear object masses for the F06, BGP07 and GS09 data are given by the respective authors as 45 per cent, 25 per cent and a factor of 2 respectively. In passing we note that if NCs are related to ultra compact dwarf galaxies (e.g. Kroupa et al. 2010) they may have a high stellar  $M/L$  due to either a bottom-heavy (Mieske et al. 2008) or top-heavy initial mass function (Dabringhausen et al. 2009).

BGP07 distinguish between extended nuclear components (11 objects) and unresolved nuclear components (also 11 objects — 5 galaxies contain both a resolved and unresolved nuclear component), finding that the extended components are well fit with an exponential profile and are thus likely to be nuclear disks (or possibly nuclear bars), whereas the unresolved components are probably nuclear star clusters. They revealed that the disks and clusters follow quite different relations, in terms of, for example, how the nuclear disk luminosity scales with host galaxy  $\sigma$ . For this reason it is important to distinguish between nuclear disks and clusters when examining the scaling relations of nuclear objects with their host galaxy.

F06 identified three of their objects as containing small-scale stellar disks. Based on their published *HST* surface photometry we identify one further object, NGC 4550 (VCC 1619) as likely containing a nuclear stellar disk. These four nuclear disks are also the most extended nuclear components in the F06 sample, having half-light radii ranging from 26 to 63 pc (for comparison, the mean half-light radii for the F06 nuclear objects is 4 pc). This provides final samples of 77 and 15 nuclear clusters and nuclear disks, respectively, from the galaxy samples of F06, BGP07 and GS09. 5 galaxies contain both a nuclear star cluster and a nuclear disk, thus 87 unique galaxies with a stellar CMO.

### 2.2. Host galaxy and spheroid properties

We note that we were not able to obtain every galaxy and spheroid property for every object from the literature. The number of objects for which we were able to obtain a given property is indicated in Table 1. Velocity dispersions were obtained from F06, BGP07 and GS09, giving 52/77 nuclear star cluster galaxies and 15/15 nuclear disk galaxies having measured  $\sigma$ .

We obtained total apparent  $B$ -band magnitudes for all galaxies following F06. For the BGP07 and GS09 objects and our SMBH sample we obtained  $m_B$  from de Vaucouleurs et al. (1991, RC3). For the F06 objects we obtained  $m_B$  from Binggeli et al. (1985), reduced to the RC3 system using the relation given in the HyperLeda database (Paturel et al. 2003)<sup>2</sup>. To convert to absolute magnitudes we used the distances from Mei et al. (2007) for the F06 sample, and from BGP07, GS09 and Graham et al. (2011) for the corresponding galaxies. We note that this approach fails to correct for dust (see Graham & Worley 2008). We therefore also obtained

<sup>2</sup> <http://leda.univ-lyon1.fr>

TABLE 1  
NUCLEAR CLUSTER AND BLACK HOLE SCALING RELATIONS

Relation (1)	a (2)	err(a) (3)	b (4)	err(b) (5)	$\sigma_{rms}$ (6)	r (7)	N (8)	Fit (9)	Notes (10)
$M_B + 16.9, \log M_{NC}$	6.44	0.06	-0.32	0.05	0.55	-0.64	77		
$M_B + 19.9, \log M_{BH}$	8.20	0.09	-0.65	0.11	0.39	-0.81	25		E and dE only
$M_B + 19.9, \log M_{BH}$	8.13	0.13	-0.77	0.14	0.45	-0.81	25	(X Y)	E and dE only
$M_K + 20.4, \log M_{NC}$	6.63	0.07	-0.24	0.04	0.52	-0.69	57		E and dE only
$M_K + 23.4, \log M_{BH}$	8.04	0.14	-0.48	0.09	0.40	-0.70	25		E and dE only
$M_K + 23.4, \log M_{BH}$	7.81	0.13	-0.71	0.15	0.51	-0.70	25	(X Y)	E and dE only
$\log \sigma/54.0, \log M_{NC}$	6.63	0.09	2.11	0.31	0.55	0.62	52		
$\log \sigma/224.0, \log M_{BH}$	8.46	0.06	6.10	0.44	0.47	0.88	64		
$\log \sigma/224.0, \log M_{BH}$	8.46	0.06	6.13	0.45	0.47	0.88	64	(X Y)	
$\log M_{Gal,dyn}/10^{9.6}, \log M_{NC}$	6.65	0.10	0.55	0.15	0.50	0.53	42		Ex. Sb and later
$\log M_{Gal,dyn}/10^{11.3}, \log M_{BH}$	8.47	0.07	1.37	0.23	0.46	0.76	40		Ex. Sb and later
$\log M_{Gal,dyn}/10^{11.3}, \log M_{BH}$	8.51	0.07	1.55	0.26	0.50	0.76	40	(X Y)	Ex. Sb and later
$\log M_{Gal,*}/10^{9.6}, \log M_{NC}$	6.73	0.06	0.80	0.10	0.53	0.72	76		
$\log M_{Gal,*}/10^{11.3}, \log M_{BH}$	9.40	0.32	2.72	0.69	1.03	0.55	59		
$\log M_{Gal,*}/10^{11.3}, \log M_{BH}$	9.69	0.34	3.07	0.72	1.16	0.55	59	(X Y)	
$\log M_{Sph,*}/10^{9.6}, \log M_{NC}$	7.02	0.10	0.88	0.19	0.63	0.64	62		
$\log M_{Sph,*}/10^{11.3}, \log M_{BH}$	8.80	0.11	1.20	0.19	0.63	0.65	39		
$\log M_{Sph,*}/10^{11.3}, \log M_{BH}$	9.01	0.17	1.61	0.30	0.80	0.65	39	(X Y)	

Column (1):  $X$  and  $Y$  parameters of the linear regression. Columns (2)-(5): Slope  $b$  and zeropoint  $a$ , and their associated error, from the best-fitting linear relation. Column (6): Root mean square (rms) scatter in the  $\log M_{mco}$  direction. Column (7): Spearman  $r$  coefficient. Column (8): Number of data points contributing to the fit. Column (9): Fits of the form  $\log y = a + b \log x$  (or  $\log y = a + bx$  for  $M_B$  and  $M_K$ ), were performed using the BCES(ORTH) regression unless marked (X|Y) to indicate that a BCES(X|Y) regression was used.

total  $K$ -band magnitudes,  $m_K$ , for 81/87 nuclear stellar object galaxies and 62/64 SMBH galaxies from the 2 Micron All Sky Survey (2MASS) Extended Source Catalogue (Jarrett et al. 2000).

We derive dynamical masses using the simple but popular virial estimator:  $M_{dyn} = \alpha \sigma_e^2 R_e / G$ , where  $R_e$  is the effective half-light radius and  $\sigma_e$  the luminosity-weighted velocity dispersion measured within a  $1 R_e$  aperture. Following F06, we used a value of  $\alpha = 5$  for the F06 galaxy sample. The virial factor  $\alpha$  can take on a range of values (Bertin et al. 2002) depending on the radial mass distribution. By comparing virial estimator derived masses to the results of more sophisticated dynamical models, Cappellari et al. (2006) found that, in practical situations when working with real data,  $\alpha = 5$  provides a virtually unbiased estimate of a galaxy’s dynamical mass. They found this to be true for galaxies with a broad range of Sérsic indices,  $n = 2 - 10$  and bulge-to-total ratios,  $B/T = 0.2 - 1.0$ . They caution, however, that their result “strictly applies to virial measurements derived... using ‘classic’ determination of  $R_e$  and  $L$  via  $R^{1/4}$  growth curves, and with  $\sigma_e$  measured in a large aperture.” Based on their findings we conclude that the virial estimator is a reasonable approximation of the dynamical mass for galaxies of types Sa and earlier – we do not determine  $M_{dyn}$  for galaxies of morphological type Sb or later, as these are heavily disk-dominated systems for which the virial estimator has not been calibrated.

For the BGP07, GS09 and SMBH objects we use  $R_e$  values from the RC3 (which are determined from  $R^{1/4}$  curve-of-growth fits to the surface brightness profile). For the F06 objects we use  $R_e$  values from Ferrarese et al. (2006b) which are derived from Sérsic  $R^{1/n}$  fits to the observed surface brightness profile. For these 51 objects F06 report a range in  $n$  from 0.8 to 4.6 (with 78 per cent of galaxies with  $n$  in the range 1 to 2.5). We compared Sérsic-based  $R_e$ s for the subset of F06 galaxies for which RC3  $R^{1/4}$ -based  $R_{e,dev}$  were available (22 objects) and

found good agreement, with a zeropoint offset of 0.15 dex and a scatter of 0.03 dex.. For these comparison galaxies  $n$  ranged from 1.1 to 4.6 (with 72 per cent of galaxies with  $n$  in the range 1 to 2.5), representative of the full 51 objects. This suggests that, after we apply the zeropoint correction to the F06  $R_{e,s}$  ( $R_{e,corr} = 0.85 R_{e,F06}$ ), the use of Sérsic fit based  $R_e$ s will not significantly bias  $M_{dyn}$  for the F06 objects. While we find good agreement for this small sample of galaxies for the specific methods used to determine  $R_e$  by the respective authors, we caution that in general Sérsic and  $R^{1/4}$  based  $R_e$  typically show significant differences (Trujillo et al. 2001). Our velocity dispersions are determined within inhomogeneous apertures which are not true measurements of  $\sigma_e$ . We elect not to apply an aperture correction to our measurements given the broad range of velocity dispersion profiles found in early-type galaxies (Cappellari et al. 2006), and instead incorporate this into the uncertainty on our derived  $M_{dyn}$ . After excluding disk-dominated galaxies of type Sb or later we were able to derive  $M_{dyn}$  for 47/87 nuclear stellar objects and 40/64 SMBH objects; all objects for which a  $\sigma$  and  $R_e$  measurement was available. Typical errors on  $M_{dyn}$  are  $\sim 50$  per cent.

We additionally determine stellar masses for the full galaxy,  $M_{Gal,*}$ , and for the spheroidal component,  $M_{Sph,*}$ . To determine  $M_{Gal,*}$  we multiplied the total galaxy luminosity of each object by the appropriate mass-to-light ratio. For the F06 data we took total  $g$ -band magnitudes and determined mass-to-light ratios according to Bell et al. (2003) from  $g-i$  colors from Ferrarese et al. (2006b). For all other objects we used  $M_K$  from 2MASS (excluding galaxies with no 2MASS  $M_K$  total magnitude) and, following BGP07, assumed a standard mass-to-light ratio,  $M/L_K = 0.8$  (see also Bell & de Jong 2001).  $M_{Gal,*}$  was determined for 81/87 nuclei objects and 59/64 SMBH objects. All magnitudes and colors were corrected for Galactic extinction following Schlegel et al. (1998). The F06 data was addition-

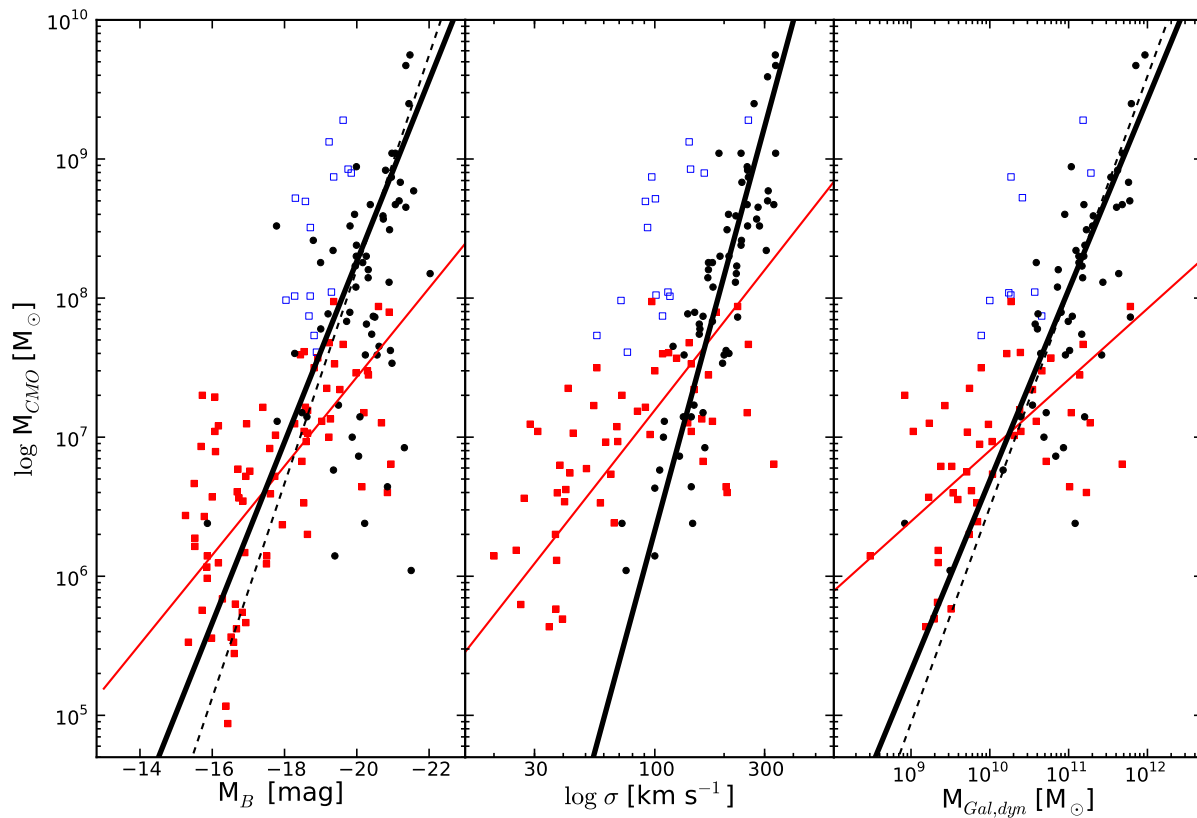


FIG. 1.—  $M_{NC}$  and  $M_{BH}$  mass vs. galaxy magnitude  $M_B$  (left panel), velocity dispersion  $\sigma$  (middle panel) and dynamical mass  $M_{Gal,dyn}$  (right panel). Black dots indicate SMBHs, red squares indicate NCs and open blue squares show those objects identified as NDs. The thick black and thin red lines indicate the best-fitting linear relations determined by the BCES(ORTH) method for the SMBH sample and the NC sample respectively. The dashed black line indicates the linear fit determined from the BCES(X|Y) method. The fit shown for the  $M_B H-M_B$  relation (black lines, left panel) is for galaxies classified E and dE only, as the fit to all galaxies was poor. We note that lower-luminosity galaxies typically lie below this relation – consistent with the bent relation found by Graham (2012a).

ally corrected for internal extinction by Ferrarese et al. (2006b). Data for other objects was not corrected for internal extinction, though we note that for most galaxies  $M_K$  and  $M/L_K$  are minimally affected by dust extinction.

$M_{Sph,*}$  was determined by multiplying the total *spheroid* magnitude of each object by the appropriate mass-to-light ratio as described above. We use the spheroid masses provided by GS09 for their galaxies. We adopt the same spheroid masses as BGP07, obtained by multiplying their *K*-band spheroid magnitudes by  $M/L_K = 0.8$ . For the F06 galaxies we use the stellar masses described above, excluding 16 galaxies classified as S0 or dS0 as they are likely to contain a large scale disk and no bulge-disk decomposition is available. For the SMBH sample spheroid magnitudes were taken from Marconi & Hunt (2003) (with the exception of NGC 2778 and NGC 4564, see Graham 2007) and Häring & Rix (2004), with optical colors obtained from the HyperLeda database. This resulted in  $M_{Sph,*}$  for 71/87 nuclear stellar object galaxies and 39/64 SMBH galaxies – all galaxies for which a spheroid mass or spheroid magnitude and an optical color were available. Typical errors on  $M_{Gal,*}$  are  $\sim 25$  per cent and on  $M_{Sph,*}$   $\sim 40$  per cent due to the increased uncertainty in separating the spheroid compo-

nent of the galaxy’s light.

Recent works by Beifiori et al. (2012), Sani et al. (2011) and Vika et al. (2012) presented new bulge-to-disk decompositions for a significant number of galaxies in our SMBH sample. We elect not to make use of these new values for now because the agreement on the bulge-to-total flux ratios between the three authors is poor and it is unclear which provides the more accurate spheroid luminosities. For example, the three authors find bulge-to-total ratios of 0.78, 0.51 and 0.36 respectively for NGC 4596, with similar significant variations in spheroid luminosities. Agreement over decomposition of galaxy profiles into bulge and disk components is urgently needed if progress is to be made on the  $L_{Sph}$  and  $M_{Sph}$  scaling relations involving disk galaxies.

### 3. ANALYSIS

We use the BCES linear fitting routine of Akritas & Bershady (1996), which minimizes the residuals from a linear fit taking into account measurement errors in both the *X* and *Y* directions. We consider two different minimizations, BCES(ORTH), which minimizes the residuals orthogonal to the linear fit and BCES(X|Y) which minimizes the residuals in the direction of the host galaxy or spheroid variable.

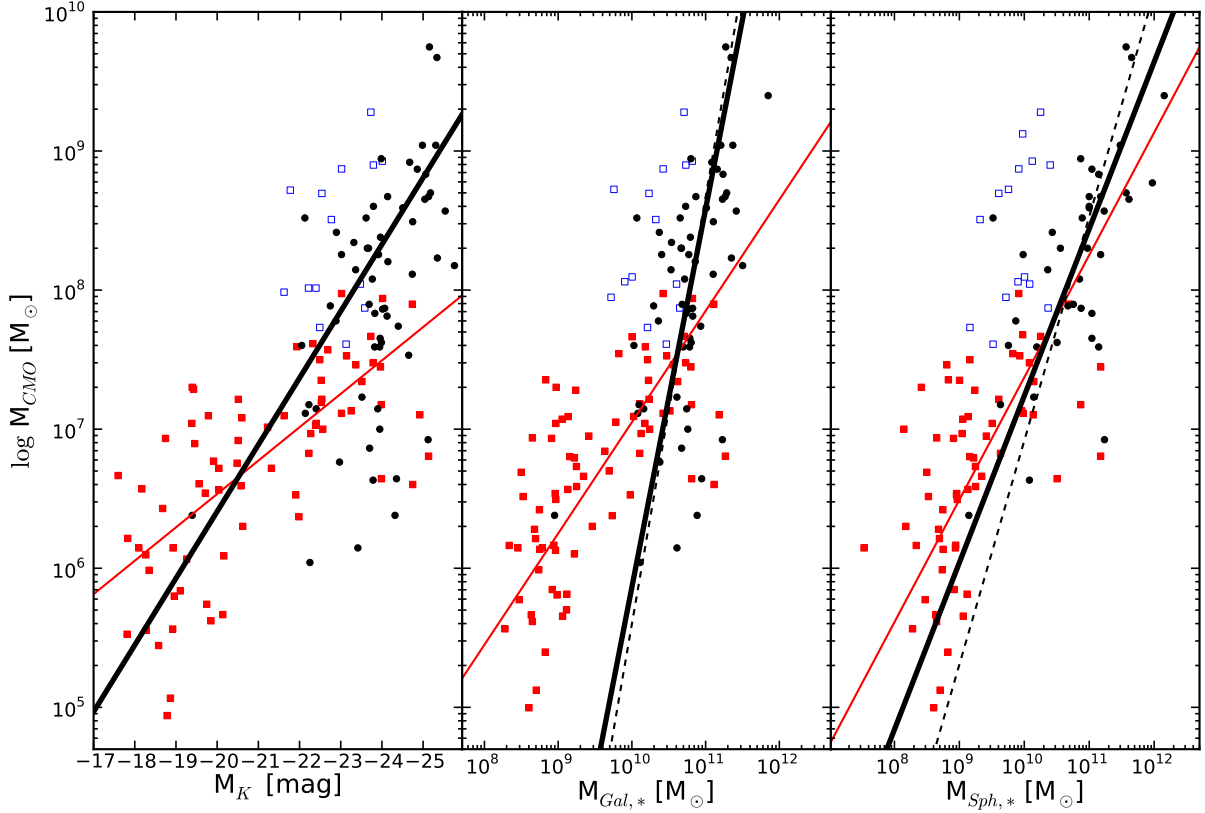


FIG. 2.—  $M_{NC}$  and  $M_{BH}$  vs. galaxy  $K$ -band magnitude,  $M_K$  (for galaxies classified E and dE only, left panel), galaxy stellar mass,  $M_{Gal,*}$  (middle panel) and spheroid stellar mass,  $M_{Sph,*}$  (right panel). Colors and symbols as in Figure 1.

Minimizing the residuals in the latter direction is the appropriate choice for the SMBH scaling relations due to the selection bias of dynamical BH mass measurements (Batcheldor 2010; Graham et al. 2011). We adopt the BCES(ORTH) minimization to facilitate comparison of the NC and SMBH relations. To compare the two scaling relations it is important to use the same minimization technique because “the different regression methods give different slopes even at the population level” (Akritas & Bershady 1996). We found that, in Monte Carlo simulations of a mock sample of NCs and SMBHs drawn from a single common CMO scaling relation, the BCES(ORTH) minimization proved most robust at recovering *the same* relation for both sets of datapoints. We therefore conclude that, to assess whether the two observed datasets are drawn from a single common scaling relation, the BCES(ORTH) minimization is the appropriate choice.

In Figure 1 we update Figure 2 from F06 by presenting linear fits of  $M_{NC}$  and  $M_{BH}$  against: host galaxy  $B$ -band magnitude  $M_B$ , velocity dispersion  $\sigma$ , and virial mass  $M_{Gal,dyn}$ . In Figure 2 we fit  $M_{NC}$  and  $M_{BH}$  against  $M_K$ ,  $M_{Gal,*}$  and  $M_{Sph,*}$ , the results of which are shown in Table 1. Our fits include galaxies which host both a NC and an SMBH – whether it is appropriate to exclude these 15 objects is debatable and discussed in Section 4.2 below. In general, including the dual-nuclei GS09 data flattens all of the NC scaling relations, but does not

significantly affect our main conclusions. In what follows we talk through the main results of Table 1.

We find a good correlation between  $M_{NC}$  and host galaxy luminosity in both the  $B$ - and  $K$ -band, with  $M_{NC} \propto L_K^{0.6 \pm 0.1}$ . In contrast the correlation between  $M_{BH}$  and host galaxy luminosity is poor, with Spearman  $r$  coefficients  $\sim -0.4$ . However, if we include only purely spheroidal systems (E and dE) this correlation improves markedly (Spearman  $r = -0.81$  and  $-0.70$  in the  $B$ - and  $K$ -bands respectively), which is unsurprising given that  $M_{BH}$  is known to correlate with the properties of the spheroid (e.g. Kormendy 2001; McLure & Dunlop 2002). The E and dE only fit is shown as the solid black line in Figure 1.

We also find a good correlation between  $M_{CMO}$  and  $\sigma$  for both NCs and SMBHs, with rms scatter in the vertical direction  $\sim 0.5$  dex and Spearman  $r$  of 0.62 and 0.88 respectively. The  $M_{NC}-\sigma$  relation that we find is significantly flatter than that found by F06 (both including and excluding the GS09 data points). This is in part due to the exclusion of NDs from our fits (open blue squares in all figures), which are typically an order of magnitude more massive than NCs. The  $M_{BH}-\sigma$  relation is in agreement with that given by Graham et al. (2011) whose data we have used.

The  $M_{NC} - M_{Gal,dyn}$  relation has the lowest rms scatter of any of the NC scaling relations (though it is not significantly tighter than either the  $M_{NC} - M_K$  or

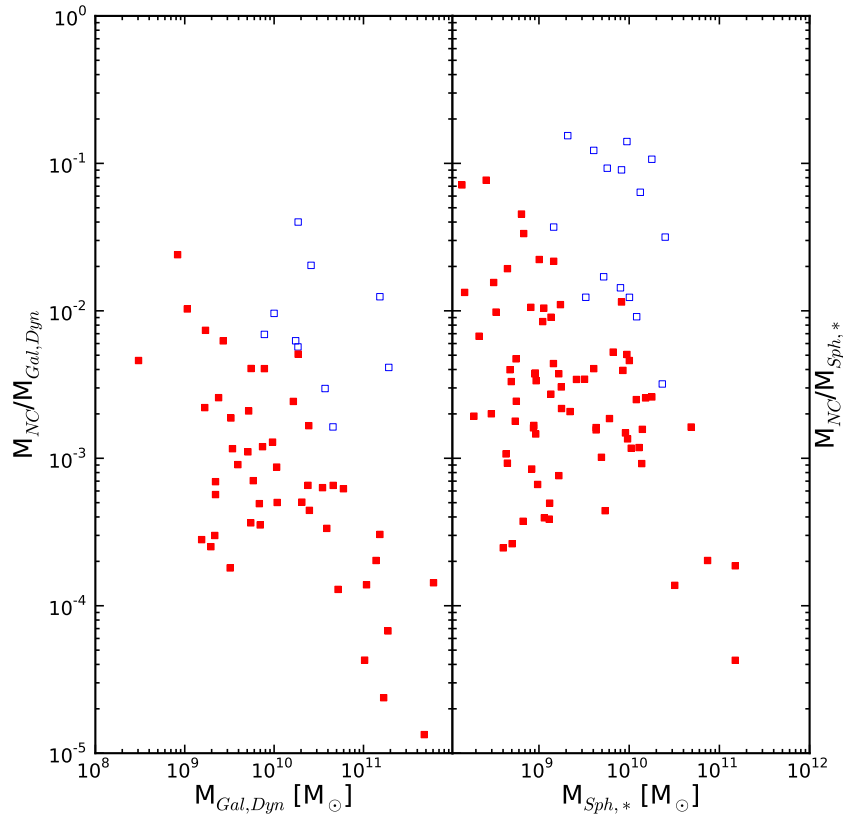


FIG. 3.— Left panel: Nuclear star cluster mass,  $M_{NC}$  as a fraction of host galaxy dynamical mass,  $M_{Gal,dyn}$  vs.  $M_{Gal,dyn}$ . Right panel: Same as left panel except using host spheroid stellar mass,  $M_{Sph,*}$ . The solid red squares indicate nuclear star clusters, the open blue squares indicate nuclear stellar disks. The left panel shows a clear trend of decreasing CMO mass fraction with  $M_{Gal,dyn}$ . While any trend is less clear with  $M_{Sph,*}$ , we find that the CMO mass fraction still spans a large range of  $\sim 2$  orders of magnitude. In both panels nuclear stellar disks (open squares) are significantly offset to higher CMO mass ratios.

$M_{NC} - M_{Gal,*}$  relations). Our  $M_{BH} - M_{Gal,dyn}$  relation is dominated by SMBHs with  $M_{BH} \gtrsim 10^8 M_\odot$ , and is consistent with previous findings in the literature (e.g. Marconi & Hunt 2003; Häring & Rix 2004). Graham (2012b) has shown that above this rough threshold the  $M_{BH}/M_{dyn}$  ratio is fairly constant, while at lower masses the  $M_{BH}/M_{dyn}$  ratio is not constant but increasingly smaller, a result which can also be seen in our Figure 1, where the datapoints fall below the extrapolation of the solid black line at lower masses, causing the steepening of our  $M_{BH} - M_{Gal,dyn}$  relation.

In agreement with BGP07, the  $M_{NC} - M_{Gal,dyn}$  relation we find is significantly flatter than the findings of F06 and WH06. The discrepancy decreases if we exclude the GS09 data points containing both NCs and SMBHs, but the slope we find is still shallower than that of F06 or WH06. This shallower slope is again primarily attributable to our exclusion of the obvious NDs from our fit.

As noted above, we have additionally examined how the NC and SMBH mass scale with the stellar mass of the host galaxy and host spheroid. As expected from the improved correlation of  $M_{BH}$  with luminosity when considering only spheroidal systems, the correlation of  $M_{BH}$  is significantly better with  $M_{Sph,*}$  than with  $M_{Gal,*}$  (the correlation with  $M_{Gal,*}$  is extremely poor and is given in

Table 1 only for completeness). This is in contrast to the  $M_{NC} - (\text{stellar mass})$  correlation, where the tighter correlation is found with  $M_{Gal,*}$  rather than  $M_{Sph,*}$ . This is consistent with the recent finding of Erwin & Gadotti (2012), though the improvement in the correlation we find is much smaller than in their work.

#### 4. DISCUSSION

##### 4.1. A common CMO-host galaxy scaling relation?

In contrast to F06 and WH06 we find that NCs and SMBHs do not follow common scaling relations. In all six diagrams that we have considered, the NCs and SMBHs appear to follow different relations (see Table 1). Our most significant finding is that (when NDs are properly excluded) the  $M_{NC} - \sigma$  relation (with a slope  $\sim 2$ ) is significantly flatter than the  $M_{BH} - \sigma$  relation (with a slope  $\sim 6$  for all galaxies, or  $\sim 5$  for E and dE galaxies: Graham et al. 2011). This is in agreement with Graham (2012b), but in contrast to F06 who find a  $M_{NC} - \sigma$  relation parallel to the SMBH relation. The difference is due to: i) the proper exclusion of NDs from our NC sample; and ii) the inclusion of NCs identified by BGP07 and GS09 that have masses higher than the SMBH/NC threshold of  $10^7 M_\odot$  suggested by WH06. NDs are significantly more massive than NCs in comparable host galaxies and follow significantly different scaling relations

(Balcells et al. 2007). Scorza & van den Bosch (1998) showed that NDs follow galaxy-scale stellar disk scaling relations, extending those relations to much lower mass.

Graham (2012a) has revealed that the  $M_{BH}$ - $M_{dyn}$  relation steepens from a slope of  $\sim 1$  at the high-mass end ( $\gtrsim 2 \times 10^8 M_\odot$ ) to a slope of  $\sim 2$  at lower masses (our slope of 1.37-1.55 is intermediate to these values because we fit a single linear relation to the high and low mass ends of this bent relation). The steepening in slope at the low-mass end is in the opposite sense to that observed for the NCs, which have a flatter slope  $0.55 \pm 0.15$  for the full sample. In the middle and right panels of Figure 1, at a CMO mass of  $\sim 10^7 M_\odot$ , NCs are, on average, found in galaxies of significantly lower  $\sigma$  and  $M_{dyn}$  than SMBHs of the same mass.

When considering the scaling of  $M_{CMO}$  with the stellar mass content of its host we find that  $M_{NC}$  appears to be driven by the total stellar mass, whereas  $M_{BH}$  is more closely associated with only the spheroidal component. Combining this finding with the result that  $M_{NC}$  follows much flatter relations with  $\sigma$  and  $M_{Gal,dyn}$  than  $M_{BH}$  does, suggests that the physical processes that lead to the build-up of a nuclear stellar cluster may be significantly different to those that drive the formation of supermassive black holes. A complementary view is provided by Figure 3, where we plot the NC mass fraction as a function of host galaxy dynamical mass and spheroid stellar mass, i.e.  $M_{NC}/M_{Gal,dyn}$  vs.  $M_{Gal,dyn}$  and  $M_{NC}/M_{Sph,*}$  vs.  $M_{Sph,*}$ . The ratio  $M_{NC}/M_{Gal,dyn}$  shows a clear trend with  $M_{Gal,dyn}$ , in the sense that the NC mass fraction decreases smoothly with  $M_{Gal,dyn}$ . Although any trend with  $M_{Sph,*}$  is less clear, we note that  $M_{NC}/M_{Sph,*}$  is not constant, spanning  $\sim 2$  orders of magnitude from 0.02 per cent to 2 per cent.

#### 4.2. Galaxies hosting supermassive black holes and nuclear star clusters

In Section 3 we noted that excluding the GS09 galaxies (which contain both a SMBH and a NC) steepened the NC scaling relations in all cases, though they still remain shallower than the corresponding SMBH scaling relations. It is likely that the SMBH and NC in these galaxies interacted in some way during their formation, hence additional physical processes may have influenced

their scaling with their host galaxy. It is unclear what exactly the result of any interaction may be: it has been suggested that (i) the presence of a single SMBH may evaporate the NC (Ebisuzaki et al. 2001; O’Leary et al. 2006), (ii) a binary SMBH may heat and erode the NC (Bekki & Graham 2010), and that (iii) some SMBHs are, in part, built up by the collision of NCs (Kochanek et al. 1987; Merritt & Poon 2004). Additionally, given the existence of some dual-CMO galaxies, it is likely that some of the supposed NC- or SMBH-only galaxies in our sample contain an undetected SMBH or NC, respectively. Because of this it is unclear whether it is correct to include or exclude the GS09 galaxies from our main NC sample. More importantly, while including the GS09 galaxies does affect the NC scaling relations our conclusions do not depend on whether we include them in our main NC sample or not.

#### 5. CONCLUSIONS

In this work we have conducted a comparison of the scaling relations for NCs and SMBHs for the largest sample of objects to date. Our principal conclusions are:

- i) The  $M_{NC}$ - $\sigma$  relation is not parallel to the  $M_{BH}$ - $\sigma$  relation when nuclear disks are properly identified and excluded and recent identifications of NCs in massive galaxies are included, in agreement with Graham (2012b).
- ii) Nuclear star clusters and black holes do not follow a common scaling relation with respect to host galaxy mass, in agreement with BGP07.
- iii) The nuclear cluster scaling relations are considerably shallower than the corresponding supermassive black hole scaling relations.
- iv) The NC mass fraction, with respect to the mass of its host galaxy or spheroid, is *not* constant, spanning  $\sim 2$  orders of magnitude. The NC mass fraction decreases in more massive galaxies.

This research was supported by Australian Research Council funding through grants DP110103509 and FT110100263.

#### REFERENCES

- Akritas, M. G., & Bershadsky, M. A. 1996, *ApJ*, 470, 706  
 Balcells, M., Graham, A. W., Domínguez-Palmero, L., & Peletier, R. F. 2003, *ApJ*, 582, L79  
 Balcells, M., Graham, A. W., & Peletier, R. F. 2007, *ApJ*, 665, 1084 (BGP07)  
 Batcheldor, D. 2010, *ApJ*, 711, L108  
 Beifiori, A., Courteau, S., Corsini, E. M., & Zhu, Y. 2012, *MNRAS*, 419, 2497  
 Bekki, K., & Graham, A. W. 2010, *ApJ*, 714, L313  
 Bell, E. F., & de Jong, R. S. 2001, *ApJ*, 550, 212  
 Bell, E. F., McIntosh, D. H., Katz, N., & Weinberg, M. D. 2003, *ApJS*, 149, 289  
 Bertin, G., Ciotti, L., & Del Principe, M. 2002, *A&A*, 386, 149  
 Binggeli, B., Sandage, A., & Tammann, G. A. 1985, *AJ*, 90, 1681  
 Booth, C. M., & Schaye, J. 2009, *MNRAS*, 398, 53  
 Bruzual, G., & Charlot, S. 2003, *MNRAS*, 344, 1000  
 Cappellari, M., Bacon, R., Bureau, M., et al. 2006, *MNRAS*, 366, 1126  
 Côté, P., Piatek, S., Ferrarese, L., et al. 2006, *ApJS*, 165, 57  
 Croton, D. J., Springel, V., White, S. D. M., et al. 2006, *MNRAS*, 365, 11  
 Dabringhausen, J., Kroupa, P., & Baumgardt, H. 2009, *MNRAS*, 394, 1529  
 de Vaucouleurs, G., de Vaucouleurs, A., Corwin, Jr., H. G., et al. 1991, *Third Reference Catalogue of Bright Galaxies*, ed. Roman, N. G., de Vaucouleurs, G., de Vaucouleurs, A., Corwin, H. G., Jr., Buta, R. J., Paturel, G., & Fouqué, P.  
 Ebisuzaki, T., Makino, J., Tsuru, T. G., et al. 2001, *ApJ*, 562, L19  
 Erwin, P., & Gadotti, D. A. 2012, *Advances in Astronomy*, 2012  
 Ferrarese, L., & Merritt, D. 2000, *ApJ*, 539, L9  
 Ferrarese, L., Côté, P., Dalla Bontà, E., et al. 2006a, *ApJ*, 644, L21 (F06)  
 Ferrarese, L., Côté, P., Jordán, A., et al. 2006b, *ApJS*, 164, 334  
 Gebhardt, K., Bender, R., Bower, G., et al. 2000, *ApJ*, 539, L13  
 González Delgado, R. M., Pérez, E., Cid Fernandes, R., & Schmitt, H. 2008, *AJ*, 135, 747  
 Graham, A. W. 2007, *MNRAS*, 379, 711  
 —. 2008, *ApJ*, 680, 143

- . 2012a, *ApJ*, 746, 113
- . 2012b, *MNRAS*, accepted
- Graham, A. W., & Driver, S. P. 2007, *ApJ*, 655, 77
- Graham, A. W., Erwin, P., Caon, N., & Trujillo, I. 2001, *ApJ*, 563, L11
- Graham, A. W., & Guzmán, R. 2003, *AJ*, 125, 2936
- Graham, A. W., Onken, C. A., Athanassoula, E., & Combes, F. 2011, *MNRAS*, 412, 2211
- Graham, A. W., & Spitler, L. R. 2009, *MNRAS*, 397, 2148 (GS09)
- Graham, A. W., & Worley, C. C. 2008, *MNRAS*, 388, 1708
- Häring, N., & Rix, H.-W. 2004, *ApJ*, 604, L89
- Hu, J. 2008, *MNRAS*, 386, 2242
- Jarrett, T. H., Chester, T., Cutri, R., et al. 2000, *AJ*, 119, 2498
- King, A. 2005, *ApJ*, 635, L121
- Kochanek, C. S., Shapiro, S. L., & Teukolsky, S. A. 1987, *ApJ*, 320, 73
- Kormendy, J. 2001, in *Astronomical Society of the Pacific Conference Series*, Vol. 230, *Galaxy Disks and Disk Galaxies*, ed. J. G. Funes & E. M. Corsini, 247–256
- Kormendy, J., & Richstone, D. 1995, *ARA&A*, 33, 581
- Kroupa, P., Famaey, B., de Boer, K. S., et al. 2010, *A&A*, 523, A32
- Magorrian, J., Tremaine, S., Richstone, D., et al. 1998, *AJ*, 115, 2285
- Marconi, A., & Hunt, L. K. 2003, *ApJ*, 589, L21
- McLaughlin, D. E., King, A. R., & Nayakshin, S. 2006, *ApJ*, 650, L37
- McLure, R. J., & Dunlop, J. S. 2002, *MNRAS*, 331, 795
- McQuillin, R. C., & McLaughlin, D. E. 2012, *MNRAS*, accepted
- Mei, S., Blakeslee, J. P., Côté, P., et al. 2007, *ApJ*, 655, 144
- Merritt, D., & Poon, M. Y. 2004, *ApJ*, 606, 788
- Mieske, S., Dabringhausen, J., Kroupa, P., Hilker, M., & Baumgardt, H. 2008, *Astronomische Nachrichten*, 329, 964
- Neumayer, N., & Walcher, C. J. 2012, *Advances in Astronomy*, 2012
- O’Leary, R. M., Rasio, F. A., Fregeau, J. M., Ivanova, N., & O’Shaughnessy, R. 2006, *ApJ*, 637, 937
- Paturel, G., Petit, C., Prugniel, P., et al. 2003, *A&A*, 412, 45
- Sani, E., Marconi, A., Hunt, L. K., & Risaliti, G. 2011, *MNRAS*, 413, 1479
- Schlegel, D. J., Finkbeiner, D. P., & Davis, M. 1998, *ApJ*, 500, 525
- Scorza, C., & van den Bosch, F. C. 1998, *MNRAS*, 300, 469
- Seth, A., Agüeros, M., Lee, D., & Basu-Zych, A. 2008, *ApJ*, 678, 116
- Silk, J., & Rees, M. J. 1998, *A&A*, 331, L1
- Trujillo, I., Graham, A. W., & Caon, N. 2001, *MNRAS*, 326, 869
- Vika, M., Driver, S. P., Cameron, E., Kelvin, L., & Robotham, A. 2012, *MNRAS*, 419, 2264
- Wehner, E. H., & Harris, W. E. 2006, *ApJ*, 644, L17 (WH06)